Journal of Food Engineering xxx (2017) xxx-xxx

Contents lists available at ScienceDirect

Journal of Food Engineering

journal homepage: www.elsevier.com

Effects of viscosity and agitation rate on temperature and flow field in cans during reciprocal agitation

Ferruh Erdogdu[a, *], Mustafa Tutar[b, c], Fabrizio Sarghini[d], Dagbjorn Skipnes[e]

[a] Department of Food Engineering, Ankara University, Ankara, Turkey
[b] Mechanical and Manufacturing Department, MGEP Mondragon Goi Eskola Politeknikoa, Spain
[c] IKERBASQUE, Basque Foundation for Science, Spain
[d] University of Naples Federico II, Department of Agricultural Sciences, Naples, Italy
[e] Department of Process Technology, Nofima AS, Norway

ARTICLE INFO

Article history:
Received 20 November 2016
Received in revised form 26 May 2017
Accepted 28 May 2017
Available online xxx

Keywords:
Reciprocal agitation
Viscosity effects
Canning
Optimization

ABSTRACT

A new canning process with a reciprocal agitation has been introduced recently. In this process, agitation with rapid back and forth motion of containers increases heat transfer rate by imposing additional external forces. In this process, balance between reciprocal agitation and buoyancy and viscous forces enable shorter process time leading to increased quality retention due to the considerable increase in temperature. Viscous forces are additional to affect this balance. Therefore, the objectives of this study were to determine the effect of viscosity on the evolution of temperature and flow field in a reciprocal agitation system and to determine the optimum agitation rates. For this purpose, an experimentally validated multi-phase model developed in a non-inertial reference frame of moving mesh was used. The simulations were carried out for a 98.2 × 115 mm can containing distilled water (low viscosity Newtonian case) and high viscosity non-Newtonian liquids with 2% headspace at reciprocal agitation rates from 20 to 140 rpm. An optimum agitation rate was calculated based on the change in Froude and Taylor numbers to compare agitation effects with gravitational and viscous effects. A significant effect of viscosity on temperature distribution was also presented. The results of this study might be used to optimize the process for improving retention of nutrients and health-promoting compounds of processed foods.

Nomenclature

c_p	Specific heat, J/kg-K
E_r	Relative internal energy, J/kg
Fr	Froude number
$\vec{F}$	External body force, N
H_r	Relative total enthalpy, J/kg
I	Unit tensor
k	Thermal conductivity, W/m-K
k	Turbulence kinetic energy value, m^2/s^2
L	Length of the connectivity rod in the reciprocal agitation system, m
n	Aspect ratio of the reciprocal agitation system
P	Static pressure, Pa
R	Radius of the crank in the reciprocal agitation system, m
S_h	Source term, W/m^3
t	Time, s
T	Temperature, K
Ta	Taylor number
$\vec{u}_r$	Longitudinal velocity of the moving mesh, m/s
v	Tangential velocity, m/s
$\vec{v}_r$	Relative velocity vector of a fluid cell, m/s
x	Displacement in the reciprocal agitation system, m

Greek letters

β	Volume expansion coefficient, 1/K
ε	Turbulence dissipation rate, m^2/s^3
$\dot{\gamma}$	Shear rate, 1/s
μ	Dynamic viscosity, Pa-s
ρ	Density, kg/m^3
$\bar{\bar{\tau}}_r$	Stress tensor, N/m^2
ω	Reciprocal agitation rate, rad/s

1. Introduction

Canning, processing of food products in hermeticlally closed containers, has been a convenient and economic way to provide safe and shelf stable products. Static retorts with steam, water, steam/air, raining and spray water mechanisms have been widely used in canning (Ates et al., 2014). To increase the heat transfer rate, enable uniform temperature distribution in the cans and reduce process time for liq-

* Corresponding author.
Email address: ferruherdogdu@ankara.edu.tr, ferruherdogdu@yahoo.com (F. Erdogdu)

http://dx.doi.org/10.1016/j.jfoodeng.2017.05.030
0260-8774/

uid and liquid foods containing solid particles, axial rotaion and rotary retorts with end-over-end principle have been introduced and used in processing since 1920s. Introduction of axial and end-over-end rotating systems was due the slow heat penetration observed in the cans (Rosnes et al., 2011). Heat transfer for the still case (without any rotational effect) was just due to the evolution of the natural convection inside the cans, and mixing of the contents was also limited. This led to a lack of consistency in sensory and nutritive properties (Ohlsson, 1980), and rotating systems were introduced to increase heat transfer rate with mixing. However, both rotational and end-over-end retorts had a limitation of that the applied inertial forces to enable the motion within the container were in a balance between gravity and centrifugal forces (Walden and Emanuel, 2010). This balance resulted in a limited effect of agitation where heat transfer rate was increased up to a maximum, and viscosity had a certain effect on obtaining the optimal heat transfer rate (Sarghini and Erdogdu, 2016). Tutar and Erdogdu (2012) presented a detailed analysis to compare gravitational and centrifugal forces with viscosity effects during axial rotation of horizontal cans. Sarghini and Erdogdu (2016) applied this analysis to evaluate the effect of rotation rate in an end-over-end canning process.

For a more effective heat transfer rate that might be obtained with agitation, a reciprocating horizontal agitation based on moving the containers in an oscillating motion with high frequency longitudinal mechanism has been proposed, and a reciprocal agitation retort was first developed in 2006 (Ates et al., 2014). Reciprocal agitation applies horizontal reciprocation besides the effects of gravitational force. Sum of these forces is expected to enable a considerable increase in heat transfer rates in theory (Walden and Emanuel, 2010). Various experimental studies in these systems were carried out to show the improvement in heat transfer and process time (Bermudez-Aguirre, 2013a,b; Ates et al., 2013; Singh et al., 2015a,b; Singh and Ramaswamy, 2015a,b; Singh et al., 2016). Besides, Singh and Ramaswamy (2015b) presented the effect of orientation of containers during reciprocating agitation (where horizontal orientation was demonstrated to be effective for liquid products while vertical rotation was for particulate products), and Singh and Ramaswamy (2016) focused on optimizing the reciprocating intensity.

Thermal processing during reciprocal agitation might be accepted to be a thermal-vibrational convection or forced convection heating of liquid subjected to horizontal oscillations. Liffman et al. (1997), Tao et al. (2007) and Pesch et al. (2008) presented the theoretical mechanism of convection in fluid layers subjected to horizontal acceleration – shaking and heating from below. Erdogdu et al. (2016) developed a multi-phase model using finite volume method based on discretization of governing equations for liquid and gas phases in a non-inertial reference frame of moving mesh. This model was experimentally validated, and the optimal shaking rate of a reciprocal agitation system for liquid foods was determined using the changes in Froud (Fr – ratio of reciprocal agitation – inertial force to gravitational force) and Taylor (Ta – ratio of reciprocal agitation – inertial force to viscous force).

For rotation or reciprocal agitation process, heating behavior of the product is strongly dependent upon the viscosity and rotation/agitation rate. The changes in Fr and Ta numbers through the process compare the effects of inertial to gravitational and inertial to viscous forces. A significant effect of viscous forces compared to the rotational/centrifugal and buoyancy forces was also reported by Tutar and Erdogdu (2012). It was demonstrated that the force balance indicated by Fr and Ta numbers resulted in the heat transfer mechanism to change from convection to conduction via the negative effect of increased rotational force and viscous effects. For rotation and end-over-end rotation cases, after a certain rotation rate when the centrifugal – rotational and gravitational buoyancy forces are equal, heat transfer rate starts getting affected negatively, and viscosity is the main physical property to drive this force balance. For the case of reciprocal agitation processes, however, there was no study reported to demonstrate the effect of viscous forces – viscosity on determining temperature and flow field evolution to possibly determine an optimal agitation rate.

Therefore, the objectives of this study were to evaluate the effect of viscosity on temperature and flow evolution in the liquid canned products and to determine the optimal reciprocal agitation rate in a reciprocal agitation system using a previously developed and experimentally validated computational model.

2. Materials and methods

A previously developed (using Ansys Fluent V15, Ansys, Inc., Canonsburg, PA, USA) and experimentally validated computational model (Erdogdu et al., 2016) were used to determine the effects of reciprocal agitation rates and viscosity on temperature evolution. For this purpose, 98.2 × 115 mm sized cans were again used in the simulations. Among the thermo-physical properties, viscosity is significant to affect the evolution of temperature and flow field inside the cans. Ghani et al. (1999); Sakai et al. (2004) demonstrated the effect of temperature variable viscosity on the natural convection heating of canned foods. To test the effect of viscous forces, the cans were assumed to contain a certain (2%) headspace (air) and be filled either with distilled water or with a solution of water and 1.5% (w/w) carboxymethylcellulose (CMC). Distilled water and 1.5% CMC were considered as an example of a Newtonian and non-Newtonian liquids to represent two extreme rheological cases that can be encountered in an industrial canning processes. In both cases, presence of a 2% headspace as a possible industrial practice was considered and located on the top of the horizontally laying cans.

2.1. Computational model

In the model development, first the displacement of the can with the slider-crank derived mechanism (Fig. 1a – modified from Reader and Hooper, 1982) and tangential velocity were defined with respect to agitation rate and time as a function of the crank radius of the reciprocally agitated system:

$$x = \left[r - r\cdot(1-\sin(\omega\cdot t)) + n\cdot\left(1-\left(1-\frac{\cos^2(\omega\cdot t)}{n^2}\right)^{0.5}\right)\right]$$
$$x = [R\cdot\sin(\omega\cdot t)] \quad (1)$$

Where n is the aspect ratio$\left(n=\frac{L}{R}\right)$, x is the displacement (m),ω is the reciprocal agitation rate (rad/s), t is the time (s), R was the crank radius of the system (0.075 m), and L is the length of the connectivity rod (0.5 m). The values of 0.075 and 0.5 m for R and L were used in the experimental validation of the computational model as also extensively explained by Erdogdu et al. (2016). Since($n^2 >> \cos^2(\omega\cdot t)$) , this equation was revised with its simplified form (Eq. (1)). The larger aspect ratio (L >> R) case was also investigated in the heat transfer literature (Tao et al., 2007). This approach is valid especially for industrial applications since lateral dimension would be larger than the layer R. Even though the first derivation of the revised – simplified version of Eq. (1) resulted in a `cosine' oscillation in the

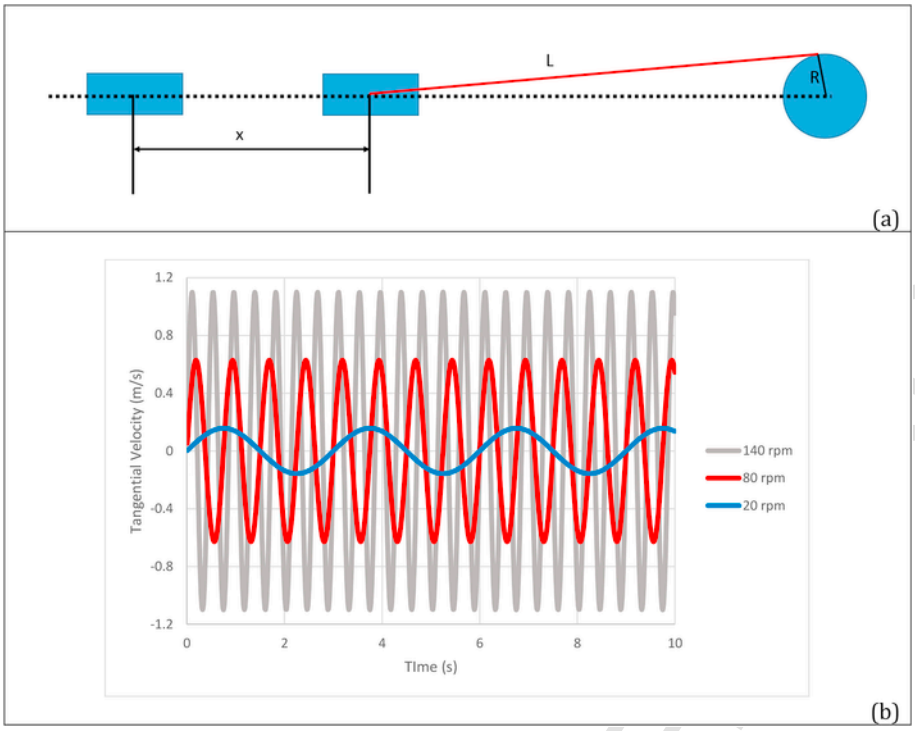

Fig. 1.

tangential velocity (v = R·ω·cos(ω·t)), it brings a non-zero velocity issue initially(t→0), which would not be a possible case to start the process. Therefore, the oscillation was displaced with one period to enable the use of Eq. (2) (Erdogdu et al., 2016):

$$\begin{aligned} &v = R\cdot\omega\cdot\sin(\omega\cdot t)\\ &\lim_{t\to 0} v = 0 \end{aligned} \tag{2}$$

The tangential velocity change at 20, 80 and 140 rpm is shown in Fig. 1b.Governing equations:

Continuity and momentum conversation equation were for time averaged flow variables of a compressible fluid in a non-inertial frame:

$$\frac{\partial \rho}{\partial t} + \nabla \rho \vec{v}_r = 0 \tag{3}$$

$$\frac{\partial}{\partial t}\left(\rho \vec{v}_r\right) + \nabla\left(\rho \vec{v}_r \vec{v}_r\right) = -\nabla P + \nabla \bar{\bar{\tau}}_r + \vec{F} \tag{4}$$

where $\vec{v}_r$ was the relative velocity vector of a fluid cell (m/s),ρ was the density (kg/m^3), P was the static pressure (Pa), t was the time (s), $\vec{F}$ was the external body force (N) for gravitational and acceleration effects in the non-inertial frame motion. The stress tensor, $\bar{\bar{\tau}}_r$was:

$$\bar{\bar{\tau}} = \mu\left[\left(\nabla \vec{v}_r + \nabla \vec{v}_r^{\,T}\right) - \frac{2}{3}\nabla \vec{v}_r I\right] \tag{5}$$

whereμ was the dynamic viscosity (Pa.s), I was the unit tensor, and the second term on the right hand side was the effect of volume dilation, which was assumed to be negligible since it had no effect in the process. This assumption of negligible volume dilation $\left(\nabla \vec{v}_r = 0\right)$ was due to the incompressible fluid approach in the simulations. Energy conservation equation was used in terms of relative total enthalpy(H_r) and relative internal energy(E_r):

$$\frac{\partial}{\partial t}\rho E_r + \nabla\left(\rho \vec{v}_r H_r\right) = \nabla\left(k\nabla T + \bar{\bar{\tau}}_r\right) + S_h \tag{6}$$

Where

$$H_r = E_r + \frac{P}{\rho} \tag{7}$$

$$E_r = h - \frac{P}{\rho} + \frac{1}{2}\left(v_r^2 - u_r^2\right) \tag{8}$$

Velocity evolutions, due to the moving mesh of the oscillatory reciprocating motion, were transformed from stationary to rotating frame:

$$\vec{v}_r = \vec{v} - \vec{u}_r \tag{9}$$

where$\vec{v}$ was the absolute velocity of the stationary frame (m/s) and $\vec{u}_r$ was the longitudinal velocity of the moving mesh (m/s).Thermal – physical properties:

All the required thermal and physical properties for air and water were based on temperature dependent polynomial functions (Tutar and Erdogdu, 2012) while the following values were used for 1.5% CMC case, as also reported by Sarghini and Erdogdu (2016):

- Thermal conductivity (k): 0.7 W/m-K,
- Specific heat (c_p): 4100 J/kg-K,
- Density (ρ):1030 kg/m^3 (to apply the Boussinesq approach, the volume expansion coefficient (β) of 0.0002 1/K was used)

Viscosity of 1.5% CMC solution, however, was described using a power law model. To prevent the convergence problems due to the strong asymptotic behavior at low shear rates, a cut-off shear rate value of 0.1 s^{-1} was set. This choice was adopted to consider the creep behavior which is not represented in a power law model: in numerical solution of non-Newtonian fluids very low shear rate zones (for example in corners) can appear, and the exponentially growing viscosity for $\dot{\gamma} \to 0$ introduces unphysical viscosity values.

The temperature dependence was modeled using the approach described by Sarghini et al. (2016) adopting a local quadratic Taylor expansion (also to reduce numerical interpolation errors) for temperature:

$$\mu(T, \dot{\gamma}(x)) = \mu_0(T, \dot{\gamma}(x)) + \sum_{n=1}^{3} \left(\frac{\partial^n \mu(\dot{\gamma})}{\partial T^n} \right) \frac{(T - T_{ref})^n}{n!} \quad (10)$$

where x was the coordinates vector, and $\dot{\gamma}$ was the shear rate (1/s). Further details for implementing the temperature and shear rate dependence of this non-Newtonian case were reported by Sarghini et al. (2016) and Sarghini and Erdogdu (2016). The temperature dependence of consistency (from 19.7 to 2.08 Pa.s^n from 30 to 90 C) and flow behavior index (n: from 0.37 to 0.59 from 30 to 90 C) for the 1.5% CMC – the non-Newtonian case were provided by Abdelrahim et al. (1994). The rheology for the CMC solutions were focused in the literature by also Vais et al. (2002); Cancela et al. (2005); Yang and Zhu (2007); Li et al. (2012).

For the case of water, turbulent flow simulations were applied (for Rayleigh number over 2.6E9) while laminar flow assumption was used for 1.5% CMC simulations. For turbulent cases, initial turbulence intensity (I) was assumed to be 5%, and based on the maximum possible tangential velocity (1.1 m/s - based on Eq. (4) at 140 rpm), turbulence kinetic energy value (k) and turbulence dissipation rate (ε) were 0.00453 m^2/s^2 and 0.025 m^2/s^3:

$$k = \frac{3}{2} \cdot (v_{max} \cdot I)^2 = 0.00453 \quad (11)$$

$$\varepsilon = C_\mu^{\frac{3}{4}} \cdot \frac{k^{\frac{3}{2}}}{L} = 0.025 \quad (12)$$

Where L and C_μ were turbulent length scale (0.002 m) and turbulence model constant (0.09), respectively. Surface tension force between gas (air) and liquid phases along the interface was set to be 0.072 N/m (Lee et al., 2012). 2 and 4 min of process for Newtonian and non-Newtonian cases were simulated.Initial and boundary conditions:

The simulations were carried out using the following initial and boundary conditions:

- Initial temperature of the can was assumed to be 300 K where the can was still in a horizontal position,
- Medium temperature was 393.15 K with an infinite heat transfer coefficient,
- Effect of can wall on the heat transfer was considered to be negligible due to its high thermal conductivity value and thickness,
- No-slip condition was applied over the can walls,
- Reciprocal agitation rates of 20–140 rpm were applied with a control case of still can (0 rpm),

2.2. Numerical solution

As described by Yakhot and Orszag (1986), the governing equations were discretized together with transport equations (in the turbulent simulations for water-air Newtonian cases) using the finite volume method (FVM) combined with an interface tracking for air-liquid system. Tracking of the interface was carried out through the volume of fluid (VOF) method (Hirt and Nichols, 1981) applying Ubbink's compressive interface capturing scheme for arbitrary meshes (CICSAM - Ubbink and Issaa, 1999). In this approach, the momentum equations were shared by both fluids (air and liquid), and their volume fractions were tracked. Two-phase volume of fluid (VOF) approach with the finite volume method was utilized to simulate the dynamic monitoring of headspace and liquid (water or 1.5% CMC) and solve fluid – thermal energy interactions in a 3D computational geometry. Fig. 2 shows the computational geometry with mesh structure (Fig. 2a) and two phases of air and liquid (Fig. 2b –distribution of liquid and gas phases in xy and yz cross-sections and in the whole volume). For the numerical solution of this complex system, a finite volume method (FVM) based solver (Ansys Fluent V15, Ansys, Inc., Canonsburg, PA, USA) was used by employing the collocated FVM. The time step applied in all the simulation cases was set to10^{-4} s to assure convergence with a mesh resolution of 199728 cells. The use of this resolution was due to the previous validation study where a mesh independency study was performed with 199728–337800 mesh cells tested. Based on this experimentally validated computational model (Erdogdu et al., 2016), the following simulation schemes were applied in a pressure based solver with absolute velocity formulation solver:

- The transient formulation was first order implicit, and spatial discretization for gradient was Green-Gauss node based; for pressure PRESTO; for momentum first order upwind (or QUICK for non-Newtonian simulations); for volume fraction CICSAM (or Modified HRIC for non-Newtonian simulations); and for turbulence kinetic energy first order upwind (only for Newtonian simulaitons) with Second Order Implicit transient formulation, and
- The pressure-velocity coupling was done with a pressure implicit with splitting of operator PISO (for Newtonian) or SIMPLE for non-Newtonian simulations) scheme with skewness-neighbour coupling.

2.3. Simulations

The simulations were carried out for the reciprocal agitation rates ranging from 20 to 140 rpm. In the reciprocal agitation systems, a crankshaft is used to derive the horizontal oscillation motion reciprocally. In the development of the computational model, the angular velocity was related to the revolutions per min (rpm) as explained in detail by Erdogdu et al. (2016). With the applied time step of 10^{-4} s to assure convergence with the given mesh resolution, the required computational time to complete 5 s of the process was around 4 days in a workstation with intel Xeon CPU (E5-1620 v2 @3.7 GHz). Therefore, the study was based on observing a certain temperature difference to show the effect of the oscillation rates and the viscosity effects.

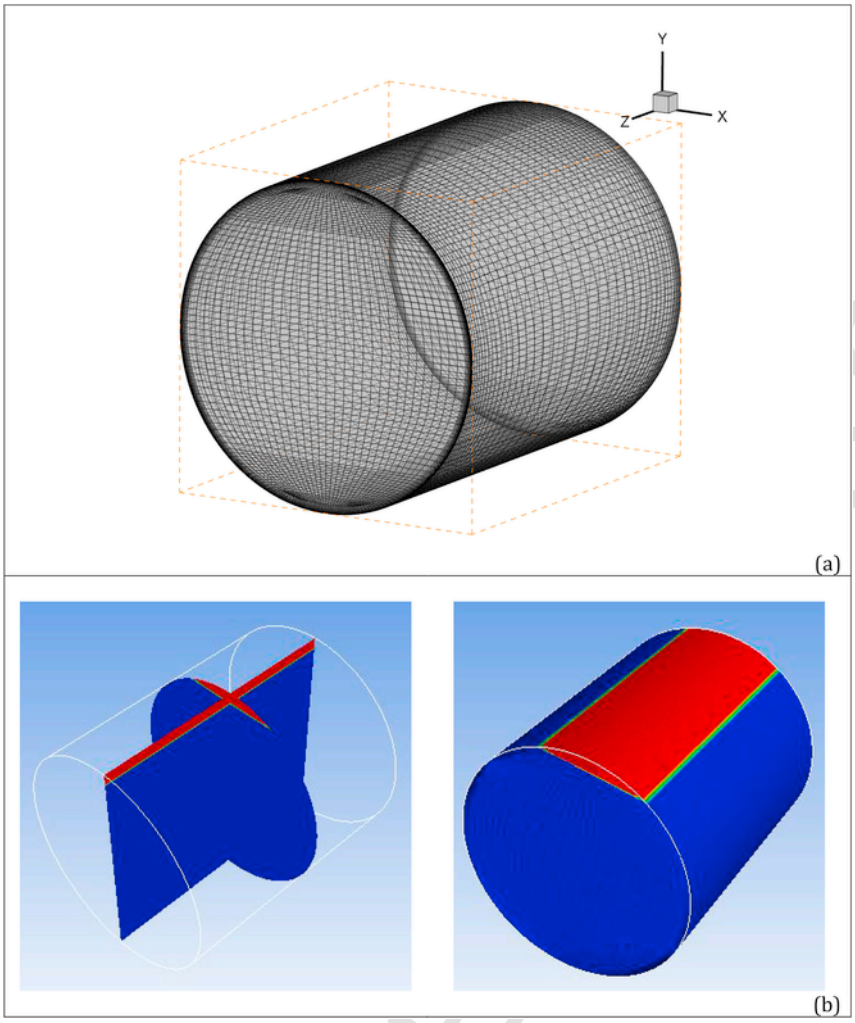

Fig. 2.

2.4. Analysis of the simulation results

As previously mentioned in the Introduction, the evolution of flow field and temperature during agitation involves interactions between agitation (inertial), gravitation and viscous forces. Therefore, a force analysis by introducing Froude (Fr) and Taylor (Ta) numbers was performed to compare the effects of the reciprocal agitation on temperature evolution. The Fr and Ta numbers are defined to be the ratio of reciprocal agitation – inertial force to gravitational and inertial to viscous forces, respectively. Based on this concept, these two modified dimensionless numbers were defined:

$$\mathrm{Fr} = \frac{f_{reciprocal-inertial}}{f_{gbf}} = \frac{\omega^2 R}{g} \tag{13}$$

$$\mathrm{Ta} = \frac{f_{reciprocal-inertial}}{f_{viscous}} = \frac{\omega^2 R^4}{\nu^2} \tag{14}$$

where f_{rbf} is the reciprocal buoyancy, f_{gbf} is the gravitational buoyancy, $f_{reciprocal}$ is the reciprocal and $f_{viscous}$ is the viscous forces, $\left(\omega = \frac{2\pi f}{60}\right)$ with f is the reciprocal agitation rate (rpm) and R was the crank radius (0.075 m) of the reciprocal agitation system, g is the gravitational acceleration (9.81 m/s^2), and ν is the volume averaged kinematic apparent viscosity of the fluid in the domain (m^2/s). The change in the Fr and Ta numbers were compared for the relative effects of reciprocal agitation, gravitation and viscous forces with respect to the temperature evolution inside the can.

3. Results and discussion

As detailed in the Simulations section, the simulations were first carried out in 98.2 × 115 mm cans including distilled water and 1.5% (w/w) CMC with 2% air (headspace) subjected to the reciprocal agitation rates of 20, 80 and 140 rpm. The stationary case of 0 rpm was also carried out for both cases to make a comparison and to demonstrate the effect of reciprocal agitation on the temperature field. The results were analyzed with respect to the temperature evolution and the change in Fr and Ta numbers to explain the effect of agitation rate on the temperature changes.

3.1. Newtonian case (water – air)

The volume averaged temperature change in the computational geometry for water - air case at the reciprocal agitation rates from 0 to 140 rpm were shown in Fig. 3. For Newtonian cases, a significant effect of reciprocal agitation rate were observed. This effect increase while the agitation rate raised from 20 to 80 rpm. Further increase of the agitation rate to 140 rpm did not make any influence on the temperature evolution.

On the other hand, effect of increased agitation on the uniformity of temperature distribution was expected. Fig. 4 shows the temperature distribution with headspace contours in the xy and yz mid cross-sections at 90 s of the process for 0, 20, 80 and 140 rpm cases. Fig. 4c–d compared to Fig. 4a–b demonstrated the effect of reciprocal agitation at 80 and 140 rpm leading to an increased temperature rate (Fig. 3) and uniformity. The lower temperature gradient obtained at 80 and 140 rpm also signified the higher mixing effects as observed at the headspace with the velocity vector fields. In Fig. 4c–d, it was recognizable that the headspace was totally disturbed at the 80 and 140 rpm agitation compared to the lower agitation at 20 rpm and natural convection case (0-rpm). Fig. 4e–f (60 s at 20 and 80 rpm, respectively – where the tangential velocity was `0′ for both cases) clearly demonstrate varying degree of mixing effects on the temperature field with the agitation rate. The higher temperature values at 80 rpm can be attributed to counter-clockwise generated stronger vortex structures which enhance the heat transfer mechanism while there are only unidirectional generated velocity vectors due to solid body motion at 20 rpm. The effect of the lower viscosity value of water should also be noted here. This enables the rather easy mixing, and this leads to an optimal agitation rate with respect to the temperture increase. This finding of an optimal agitation rate based on the temperature increase might also be significant to suggest an industrial process condition since the higher rates of agitation might result in product damage especially for the case of canned particulate food products. Singh et al. (2016) suggested a stopping criteria for the agitation after a certain temperature increase was gained to reduce the product damage.

Erdogdu et al. (2016) explained the increased rates of temperature evolution at higher agitation rates with the balance between inertial (agitation), viscous and gravitational buoyancy forces. Fr numbers (ratio of reciprocal agitation – inertial force to buoyancy forces) encountered in this study was 0.03, 0.54 and 1.64 for the agitation rates of 20, 80 and 140 rpm, respectively (Table 1). For low agitation rates, the effect of the inertial forces over buoyancy was not high but still led to a contributing effect on the temperature increase with the mixing effect. This contribution was further noticed with the increase in the agitation rates until a certain Fr number of 0.54. The change in Ta number (ratio of inertial to viscous forces), on the other hand, was also identified for each agitation rate. For 20 rpm, Ta number changed from 2.18E8 to 1.18E9 from the 1 s of the process to 100 s with a 5.41 times higher value (Table 1). This trend demonstrated the immediate effect of inertial forces over viscous forces for the Newtonian case. Its increase was more for 80 and 140 rpm processes where 6.27 (from 3.65E9 to 2.29E10) and 6.08 (1.13E10 to 6.87E10) increase was identified (Table 1).

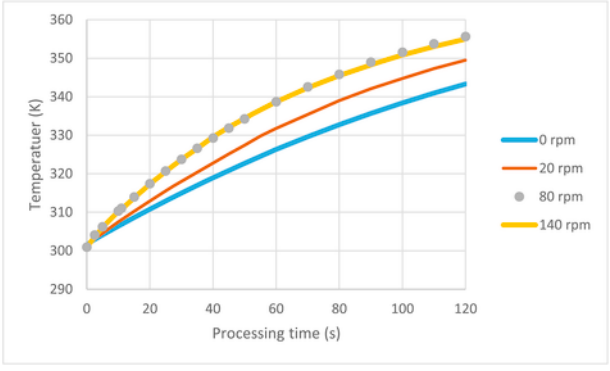

Fig. 3.

3.2. Non-Newtonian case (1.5% CMC – air)

For the non-Newtonian case, volume averaged temperature change for reciprocal agitation rates from 0 to 140 rpm was shown in Fig. 5. Fr number change was the same (0.03, 0.54 and 1.64 for the agitation rates of 20, 80 and 140 rpm, respectively) due to the same agitation rates. On the other hand, Ta number was, compared to the Newtonian case, rather low due to the higher values of viscosity. Fig. 6a shows the volume averaged apparent viscosity values encountered for non-Newtonian case as a function of process time at 0–140 rpm. The non-uniform distribution of apparent viscosity at 180 s of the process at 80 and 140 rpm was, on the other hand, shown in Fig. 6b–c. The apparent viscosity distribution is strongly linked to the strain rate values (Fig. 6d–e) whose effect (the higher the strain rate the lower the viscosity) is mitigated by the effect of temperature. In any case, significant differences of viscosity values are present pointwise. At 0 and 20 rpm reciprocation rate, the effect of temperature was dominant on the viscosity change, and the volume averaged apparent viscosity values showed a decreasing monotonic trend with increasing process time – temperature (Fig. 6a). At 80 and 140 rpm, however, oscillation effects appeared due to the dominant shear rate effects linked to the formation of internal vertical structures. The analysis of these effects requires an extensive discussion of the dynamics of the vortices formation and development during the process at high rate reciprocations.

Ta number change at 20 rpm was from 0.76 to 0.90 at 1 and 100 s (due to the decrease in the viscosity), respectively (Table 1). Even though 55.6% increase is noted, this effect on the temperature increase is not considerable. As observed in Fig. 5, there was no difference between the stationary case of 0 rpm and 20 rpm. The similar viscosity values encountered at these rates (Fig. 6) also confirmed this result. To better demonstrate the non-significant effect of reciprocal agitation at 20 rpm, temperature contours in xy and yz mid cross-sections at 180 s of the process for 0 and 20 rpm cases were shown in Fig. 7. As observed in Fig. 7a–b, there is no significant difference in the temperature contours obtained from 0 to 20 rpm cases as also shown in Fig. 5. Besides, temperature distribution at 20 rpm resembled a perfect replicate of the natural convection driven flow without any disturbance due to the reciprocal agitation. For the case at 20 rpm, the flow might be accepted to be mainly governed by the gravitational buoyancy force where the inertial force via the reciprocal agitation was negligible. Lower number of Ta number (0.76–0.90 at 1 and 100 s – Table 1) also demonstrated the effect of viscous forces over inertial forces. It might be stated that the liquid was so viscous to initiate a movement or mixing via an external force at the given reciprocation rate, and heat transfer effect was only due to the natural convection. The different pattern of the temperature evolution, compared to the Newtonian case, with respect to the agitation rates, can also be explained with the very high viscosity and approximately similar density of the non-Newtonian liquid (1.03 times higher compared to the water). This led to a less inertial force domi-

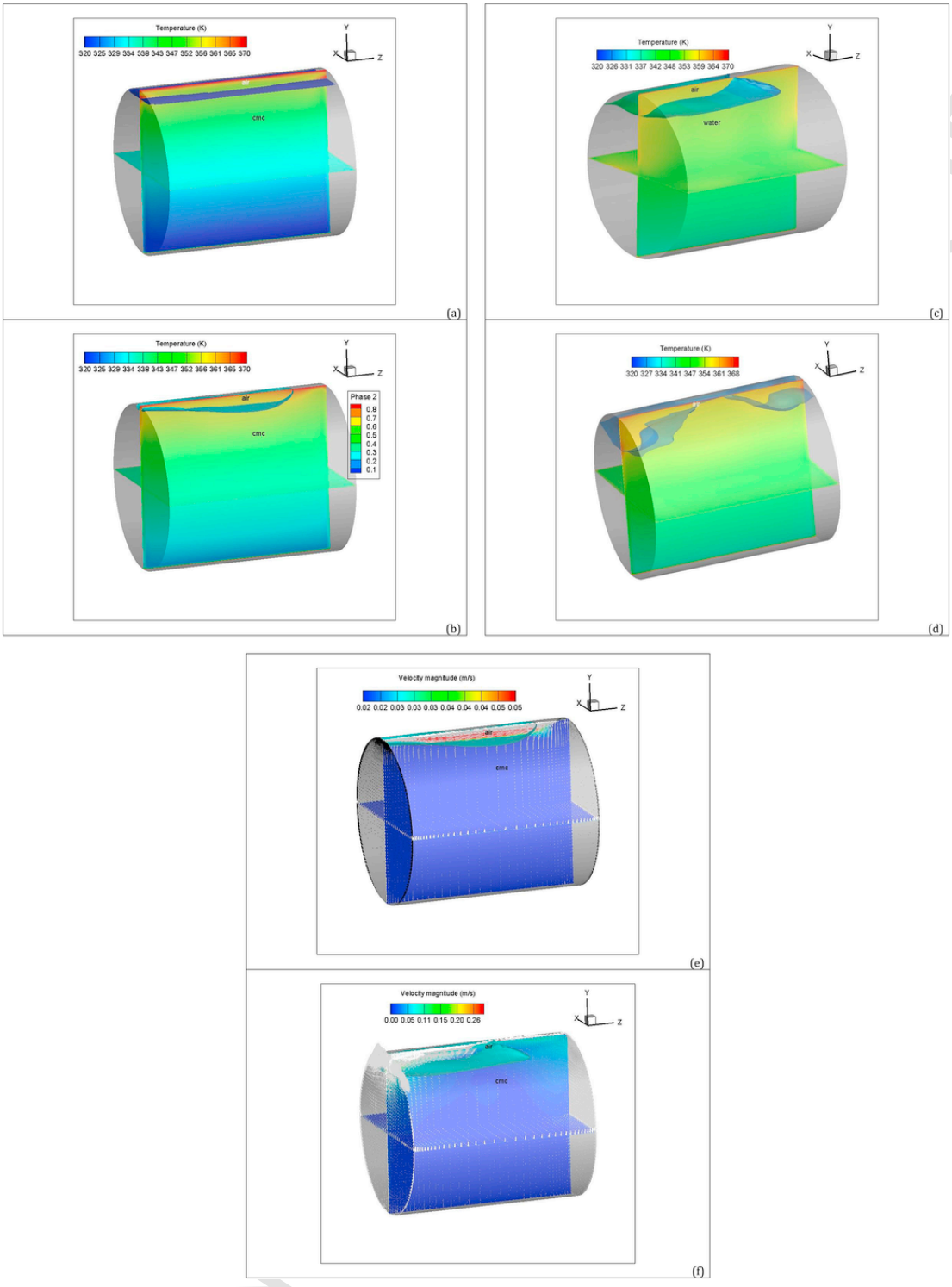

Fig. 4.

nated flow even until 80 rpm agitation rate. The magnitude of Ta number, compared to the values encountered in the Newtonian case, also demonstrated the lower effect of inertial forces over viscous forces. Even though a certain velocity magnitude was obtained until a certain agitation rate at 80 rpm, this did not lead to any mixing in the domain to make a difference on temperature distribution.

The effect of the reciprocal agitation rate on the temperature distribution at higher agitation rates (80 and 140 rpm) can be observed in Fig. 8. Fig. 8a–b shows the temperature contours in the xz and yz mid-planes at 180 s of the process at 80 and 140 rpm, respectively (the interphase between air and CMC is also shown in this figure). After 90 s of the process, the further increase of the volume averaged temperature at 140 rpm took place over 0 and 20 rpm cases (Fig. 5).

Table 1
Froude and Taylor numbers at the given oscillation rates and times.

Oscillation rate (rpm)	Froude number (Fr)	Taylor number (Ta)			
		Newtonian case		non-Newtonian case	
		t = 1 s	t = 100 s	t = 1 s	t = 100 s
20	0.03	2.18E8	1.18E9	0.76	0.90
80	0.54	3.65E9	2.29E10	10.90	15.27
140	1.64	1.13E10	6.87E10	36.85	78

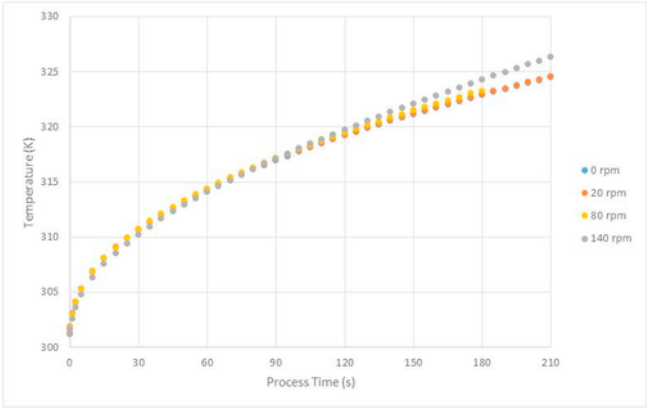

Fig. 5.

Until this point, temperature increases of all the cases from 0 to 140 rpm were very similar. As observed, the process at 140 rpm led to a rather homogeneous temperature distribution even though the volume averaged temperature distributions at these agitation rates did not differ significantly. In addition to this uniformity obtained at 140 rpm, due to the possibly intensive mixing via the inertial forces created by the reciprocal agitation, movement of the headspace was also recognizable (Fig. 8). Eventually, these distributions resulted in a very similar volume average temperature increase at these agitation rates until 90 s. Fig. 9 showed the vertical velocity contours in mid-xz and yz plane for 20 and 140 rpm at 180 s. The higher mixing effects due to the counter clockwise generated large vortex structure at 140 rpm are much more significant compared to those obtained at 20 rpm where only unidirectional solid body motion related velocity vectors are observed (the color scale was reduced by 2 order of magnitude to show significant changes at 20 rpm). These changes compared to the Newtonian case were the result of the high viscosity values encountered (Fig. 6). To further explain the effect of viscous forces over inertial forces, the changes in Ta number were used.

For 80 and 140 rpm reciprocal agitation rates, Ta number showed an increasing trend like in the case of 20. For 80 rpm, it was 10.90 at the beginning of the process (at 1 s) and changed to 13.94 and 15.27 at the 30 and 100 s of the process with a 40% increase from 1 to 100 s (Table 1) due to the decreasing trend of the volume averaged apparent viscosity where it reduced from 15.16 to 12.87 kg/m-s. For 0 and 20 rpm cases, the viscosity value was 13.08 and 13.05 kg/m-s at 85 s, respectively. At 140 rpm, on the other hand, Ta number increased from 36.85 to 78 and 111.49 at 1, 100 and 210 s of the process (Table 1). The increase at 85 s was 56%, similar to the 80 rpm case. At this point, the volume averaged apparent viscosity value reduced to 9.81 kg/m-s, and its decreasing trend continued to as low as 7.98 kg/m-s at 210 s. Until 85 s, the volume averaged temperature distribution for 80 and 140 rpm were very similar. Besides, there was no significant difference than 0 and 20 rpm cases (Fig. 5). However, following this point, the effective increase of temperature at 140 rpm was noted. This was apparently due to the increase in the Ta number where the inertial forces (via the reciprocal agitation) started showing their effect due to the higher decreasing rate in volume averaged apparent viscosity (Fig. 6). At 85 s, the viscosity value encountered at 0 and 20 rpm was 25% more compared to the 140 rpm, showing its effect against the inertial forces.

These results suggest an optimal reciprocal agitation rate for low-viscosity Newtonian case at 80 rpm with respect to the average temperature increase and temperature distribution uniformity. For non-Newtonian case, a certain inertial force should be imposed (over 80 rpm) to start gaining an effect for high viscosity which might even have possible negative effects on the temperature evolution during agitation. As demonstrated in Fig. 5, the average temperature increase due to the effect of 20 and 80 rpm agitation was very similar. The negative effect of increased viscous forces in agitated (axial rotation) processes, where the temperature increase as affected negatively with the increasing rotation rate, was encountered in the literature. Tutar and Erdogdu (2012) demonstrated this effect in axial-rotated cans. They pointed out that the increasing rotational forces in a high viscous range lead to higher centrifugal forces overcoming the gravitational forces. This prevents the natural convection, and heat transfer tends to be conduction-like with well-formed kernel-like temperature contours by slowing down the temperature increase. Sarghini and Erdogdu (2016) also identified this effect of high viscous forces in end-over-end of particulate-liquid containing cans where 6.25 rpm rotation led to higher temperature increase in the computational domain compared to the 25 rpm rotation in the initial stages of the process. For the case of this end-over-end process simulation, using the same high viscous liquid (1.5% CMC), the viscosity changes were comparatively different than the reciprocal agitation where an initial reduction was followed by an increase due to the change in the shear rate encountered during the process.

4. Conclusions

Reciprocal agitation recently demonstrated to increase the heat transfer rate in canned liquid products with additional inertial forces affecting the convection heat transfer. The increased heat transfer rate reduced process time by conserving energy and increasing the quality. However, heat transfer during reciprocal agitation in cans (like in rotational or end-over-end processing case as well) is a delicate balance between gravitational, buoyancy forces and the dynamics – viscous forces. This balance was even shown in the literature to negatively affect the temperature increase in high viscosity range since the increase in the rotational forces lead to liquid to move with a slid body motion like a solid purely conductive material. In this study, interactions between effects of viscosity and inertial forces (reciprocal agitation) were analized.

The reciprocal agitation interval (from 20 to 140 rpm) was chosen to cover a range from a low to very high agitation rate. For the low-viscosity Newtonian case, effect of reciprocal agitation rate was rather recognizable and considerable effective up to 80 rpm while further increasing the agitation rate did not make any significant contribution to heat transfer process. This was explained with the formation of vortex structures and changes in Fr and Ta numbers. For the non-Newtonian case, 20 rpm agitation rate did not affect the temperature increase of the process while higher agitation rate at 140 rpm showed its contributing effect after 85 s of the process due to the change in inertial and viscous forces (Ta number) balance with the

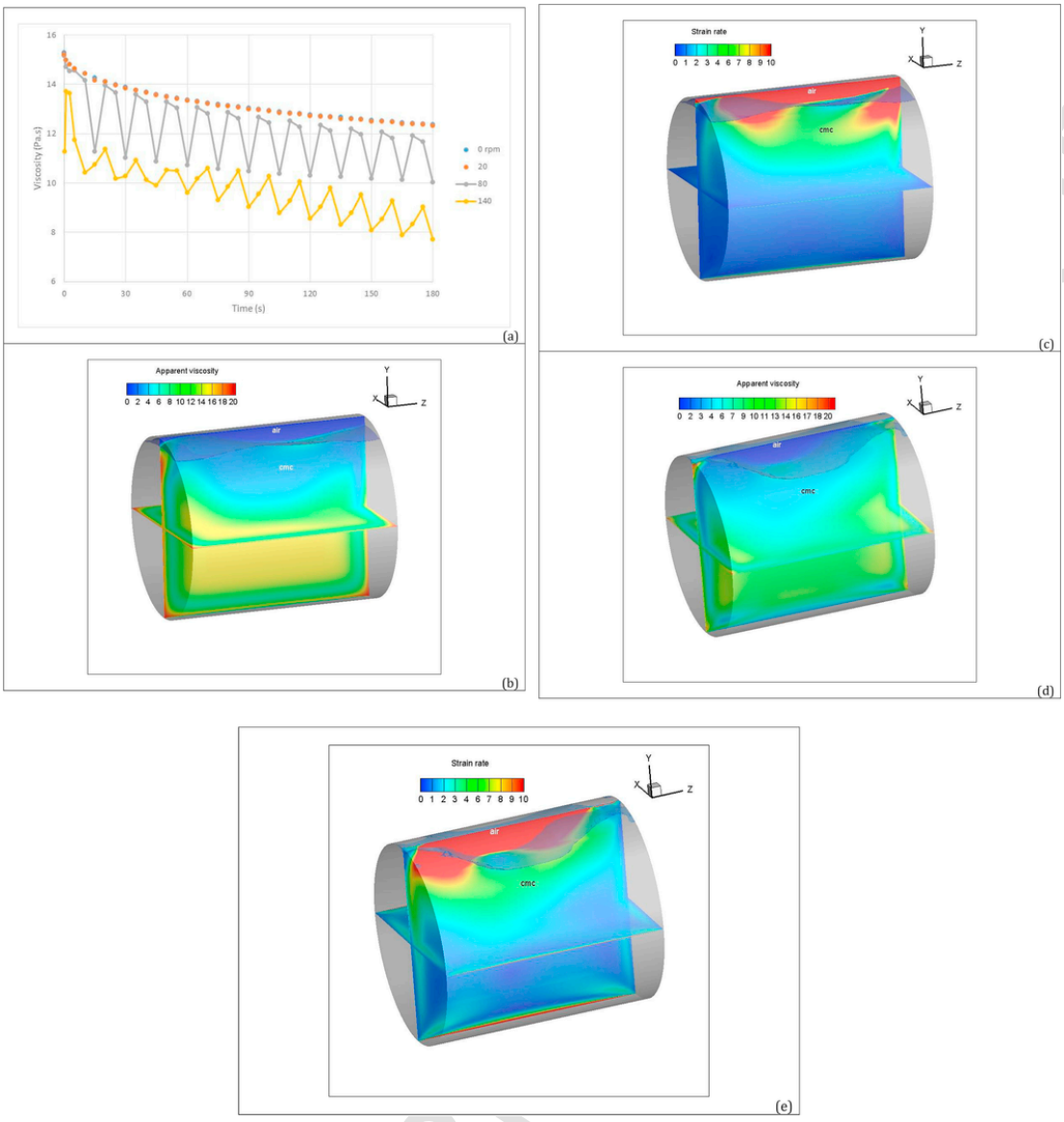

Fig. 6.

formation of counter clockwise large vortex structures and resulting mixing effects.

The results of this study demonstrated an optimum agitation rate for the Newtonian low viscosity liquids due to the balance in the gravitational, inertial and viscous forces while a different trend was observed for the high viscosity non-Newtonian case. In the latter, it was observed that a certain inertial force is required (over 80 rpm) to improve heat transfer effects in the reciprocal agitation systems.

For an industrial line to conserve energy, it might also be suggested to start the process at static conditions and then to increase the agitation rate to the optimum condition after a certain temperature attained. The results of this study might be used to optimize the process for improving retention of nutrients and health-promoting compounds of processed foods in reciprocal agitated systems including various can dimensions and relative position inside the industrial system.

The following acknowledgements are recognized by the authors:

- Ferruh Erdogdu acknowledges the Ministry of Food, Agriculture and Livestock (GDAR) of Turkey.
- Mustafa Tutar acknowledges the support from the Daniel and Nina Carasso Foundation, France (www.fondationcarasso.org) and the Department of Economic Development and Competitiveness (ELIKA).
- Dagbjorn Skipnes acknowledges the support from the Research Council of Norway through grant no. 10829.
- Fabrizio Sarghini acknowledges COST Action 15118 FoodMC for the support in the short term scientific missions.

Acknowledgement

This study was carried out within the framework of the ERA-net SUSFOOD Sunniva project, *"Sustainable food production through*

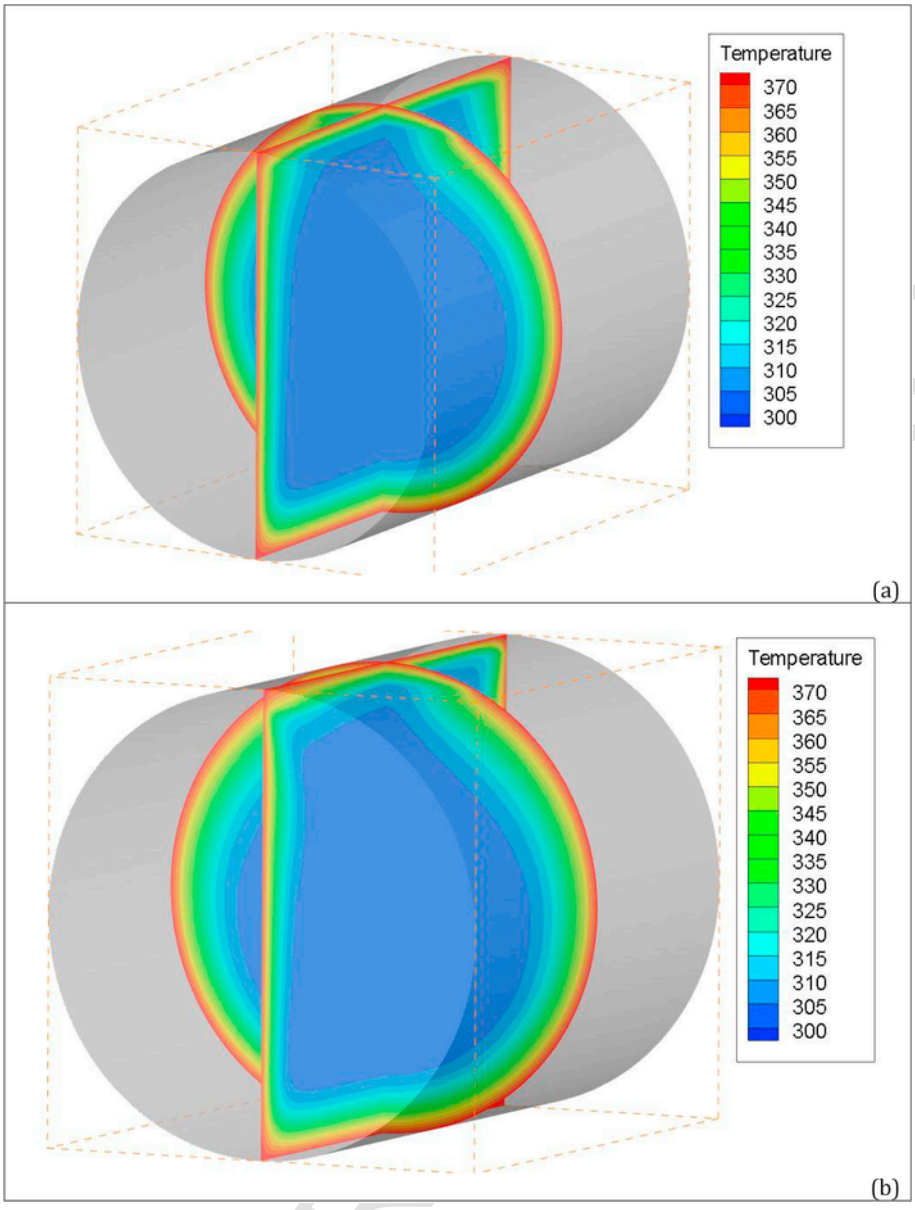

Fig. 7.

quality optimized raw material production and processing technologies for premium quality vegetable products and generated by-products".

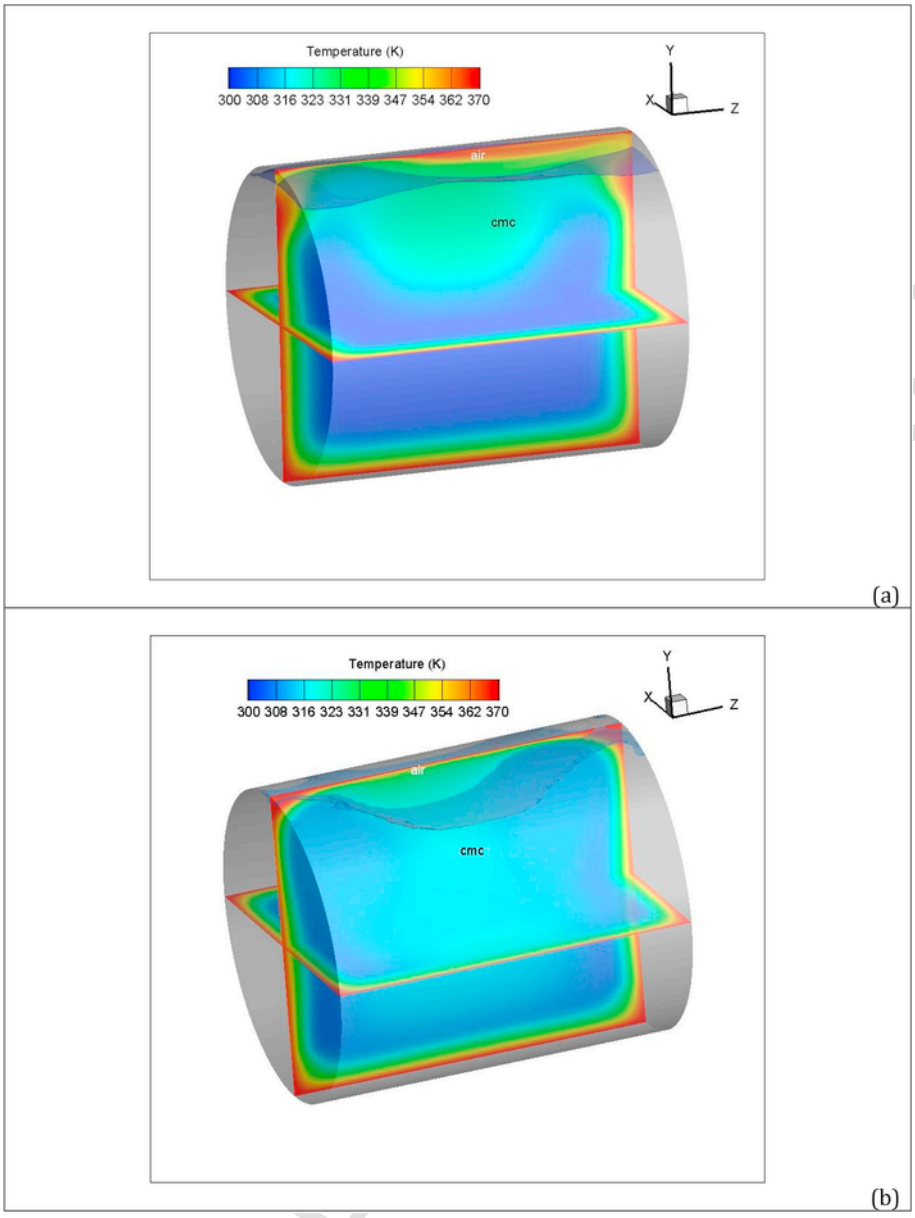

Fig. 8.

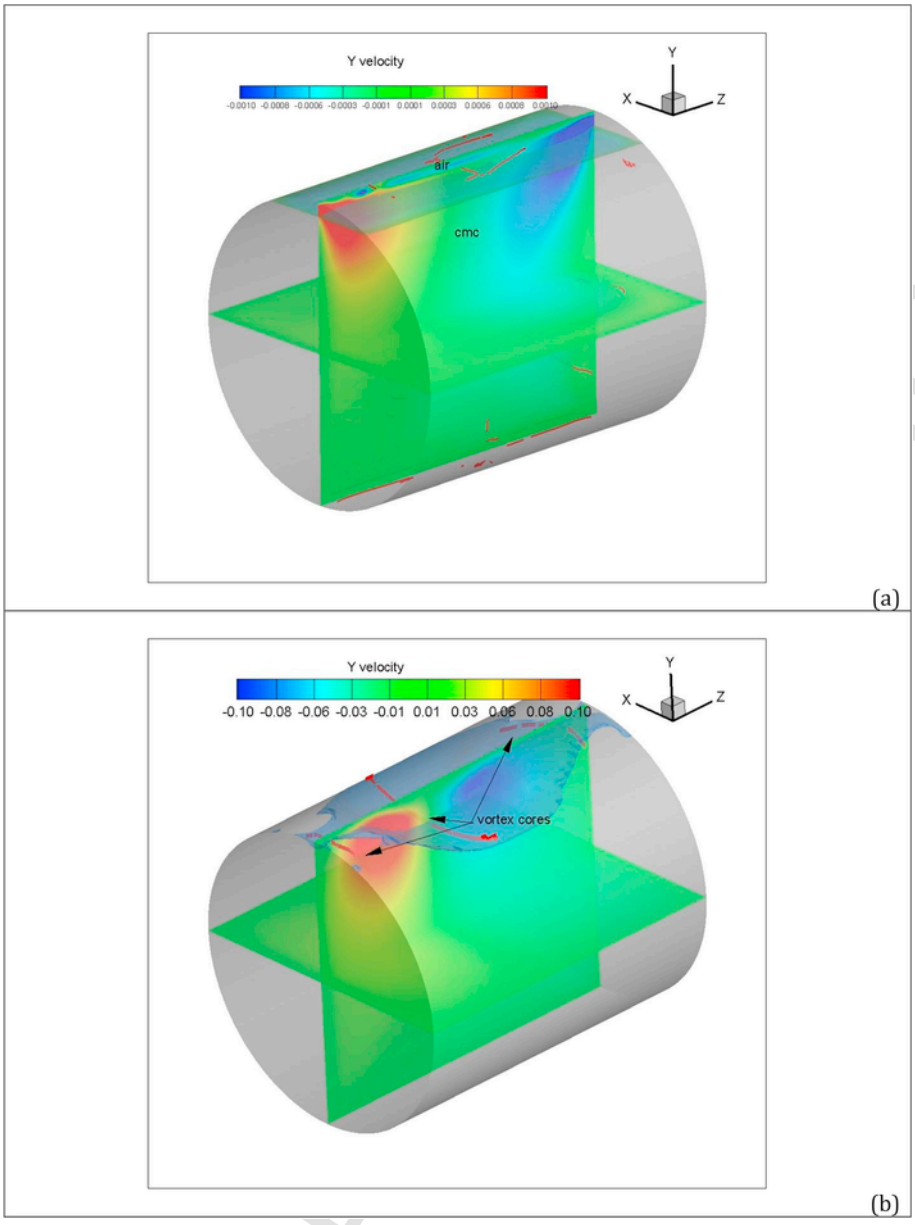

Fig. 9.

References

Abdelrahim, K.A., Ramaswamy, H.S., Doyon, G., Toupin, C., 1994. Effects of concentration and temperature on carbozymethylcellulose rheology. Int. J. Food Sci. Technol. 29, 243–253.

Ates, M.B., Skipnes, D., Rode, T.M., Lekang, O.-I., 2014. Comparison of bacterial inactivation with novel agitating retort and static retort after mild treatments. Food Control 43, 150–154.

Bermudez-Aguirre, D., Lima, F., Reitzel, J., Garcia-Prez, M., Barbosa-Canovas, G.V., 2013a. Evaluation of Total Heat Transfer Coefficient (H_T) during Innovative Retort Processing: Static, Gentle Motion and Rocking Mode. IFT Annual Meeting, Abstract number: 031–02.

Bermudez-Aguirre, D., Lima, F., Reitzel, J., Garcia-Prez, M., Barbosa-Canovas, G.V., 2013b. Development of a Mathematical Model to Describe Heat Transfer Using Three Different Processing Modes. IFT Annual Meeting, Abstract number: 031–138.

Cancela, M.A., Alvarez, E., Maceiras, R., 2005. Effects of Temperature and Concentration on Carboxymethylcellulose with Sucrose Rheology. vol. 71, 419–424.

Erdogdu, F., Tutar, M., Oines, S., Barreno, I., Skipnes, D., 2016. Determining the optimal shaking rate of a reciprocal agitation sterilization system for liquid foods: a computational approach with experimental validation. Food Bioprod. Process. 100 (Part B), 512–524.

Ghani, A.G.A., Farid, M.M., Chen, X.D., Richards, P., 1999. Numerical Simulation of Natural Convection Heating of Canned Food by Computational Fluid Dynamics. vol. 41, 55–64.

Hirt, C.W., Nichols, B.D., 1981. A computational method for pressure - surface hydrodynamics. J. Press. Vessel Technol. – Trans. ASME 103, 136–141.

Lee, B.-B., Chan, E.S., Ravindra, P., Khan, T.A., 2012. Surface tension of viscous biopolymer solutions measured using the du Nouy ring method and the drop weight methods. Polym. Bull. 69, 471–489.

Li, S., Ma, Y., Fu, T., Zhu, C., Li, H., 2012. The viscosity distribution around a rising bubble in shear-thinning non-Newtonian fluids. Braz. J. Chem. Eng. 29. 265–174.

Liffman, K., Metcalfe, G., Cleary, P., 1997. Convection due to horizontal shaking. In: CSIRO-1997: International Conference on CFD in Mineral and Metal Processing and Power Generation. pp. 165–168.

Ohlsson, T., 1980. Optimal sterilization temperatures for sensory quality in cylindrical containers. J. Food Sci. 45, 1517–1521.

Pesch, W., Palaniappan, D., Tao, J., Busse, F.H., 2008. Convection in heated fluid layers subjected to time-periodic horizontal accelerations. J. Fluid Mech. 596, 313–332.
Reader, G.T., Hooper, L.C., 1982. Stirling Engines. Spon Press, Oxfordshire, UK.
Rosnes, J.T., Skara, T., Skipnes, D., 2011. Recent advances in minimal heat processing of fish: effects on microbial activity and safety. Food Bioprocess Technol. 4, 833–848.
Sakai, N., Tang, J.W., Liu, C.M., Watanabe, M., 2004. Predicting temperature during the thermal processing of canned high-viscosity liquid food. Food Sci. Technol. Res. 10, 79–85.
Sarghini, F., Erdogdu, F., 2016. A computational study on heat transfer characteristics of particulate canned foods during end-over-end rotational agitation: effect of rotation rate and viscosity. Food Bioprod. Process. 100 (Part B), 496–511.
Sarghini, F., Romano, A., Masi, P., 2016. Experimental analysis and numerical simulation of pasta dough extrusion process. J. Food Eng. 176, 56–70.
Singh, A.P., Singh, A., Ramaswamy, H.S., 2015a. Modification of a static steam retort for evaluation heat transfer under reciprocation agitation thermal processing. J. Food Eng. 153, 63–72.
Singh, A., Singh, A.P., Ramaswamy, H.S., 2015b. A refined methodology for evaluation of heat transfer coefficients in canned particulate fluids under rapid heating conditions. Food Bioprod. Process. 94, 169–179.
Singh, A., Ramaswamy, H.S., 2015a. Effect of product-related parameters on heat-transfer rates to canned particulate non-Newtonian fluids (CMC) during reciprocating agitation thermal processing. J. Food Eng. 165, 1–12.
Singh, A.P., Ramaswamy, H.S., 2015b. Effect of can orientation on heat transfer coefficients associated with liquid particulate mixtures during reciprocation agitation thermal processing. Food Bioprocess Technol. 8, 1405–1418.
Singh, A., Singh, A.P., Ramaswamy, H.S., 2016. A controlled agitation process for improving quality of canned green beans during agitation thermal processing. J. Food Sci. 81, E1399–E1411.
Singh, A.P., Ramaswamy, H.S., 2016. Simultaneous optimization of heat transfer and reciprocation intensity for thermal processing of liquid particulate mixtures undergoing reciprocating agitation. Innovative Food Sci. Emerg. Technol. 33, 405–415.
Tao, J., Pesch, W., Busse, F.H., 2007. Convection in a fluid layer heated from below and subjected to time periodic horizontal accelerations. New Trends in Fluid Mechanics research. Shanghai, China. In: Proceedings of the Fifth International Conference on Fluid Mechanics. pp. 69–72.
Tutar, M., Erdogdu, F., 2012. Numerical simulation for heat transfer and velocity field characteristics of two-phase flow systems in axially rotating horizontal cans. J. Food Eng. 111, 366–385.
Ubbink, O., Issaa, R.J., 1999. A method for capturing sharp fluid interfaces on arbitrary meshes. J. Comput. Phys. 153, 26–50.
Vais, A.E., Palazoglu, T.K., Sandeep, K.P., Daubert, C.R., 2002. Rheological characterization of carboxymethylcellulose solution under aseptic processing conditions. J. Food Process Eng. 25, 41–61.
Walden, R., Emanuel, J., 2010. Developments in in-container retort technology: the Zinetec Shaka process. In: Doona, C.J., Kustin, K., Feery, F.E. (Eds.), Case Studies in Novel Food Processing Technologies: Innovation in Processing, Packaging and Predictive Modelling. Woodhead Publishing Ltd., Cambridge, UK.
Yakhot, H.Q., Orszag, S.A., 1986. Renormalization group analysis of turbulence. I. Basic theory. J. Sci. Comput. 1, 1–51.
Yang, X.H., Zhu, W.L., 2007. Viscosity properties of sodium carboxymethylcellulose solutions. Cellulose 14, 409–417.